

Research Article

# Ab-initio Study on Gold Doped Graphene

Nigatu Desalegn\*, Tamirat Yibika, Takele Teshome Somano

College of Natural and Computational Science Department of Physics, Wolaita Sodo University, Sodo, Ethiopia

## Abstract

This thesis investigates the electronic structure of gold-doped Graphene using first-principles calculations based on density functional theory (DFT). Employing a plane wave pseudo potential approach, the research applies generalized gradient approximations (GGA) for the exchange-correlation potential. Geometry optimization was included in all calculations to ensure complete structural relaxation, enhancing the robustness of the results. A detailed analysis was conducted to establish convergence concerning kinetic energy cutoff and k-point mesh size. Graphene showed convergence at 30 Ray, allowing for reduced computational costs, and a uniform k-point mesh of  $8 \times 8 \times 1$  was used, yielding accurate charge density and a lattice constant of 2.476 Å. Notably, the band structure reveals that two bands intersect at the K-point, indicating unique zero-gap electronic characteristics in both pure and Au-doped Graphene, which exhibit semiconductor behavior with a minimal band gap linked to the gold atom. The density of states (DOS) plot confirms no overlap at the Fermi energy or a band gap between the valence and conduction bands, solidifying grapheme's semiconducting nature. The band crossing at the Fermi level in the Au-doped Graphene super cell is particularly important, showing that the Fermi level shifts into the conduction band, with a notable DOS peak at the Fermi level indicative of strong interactions between the Au dopant and the Graphene matrix. Consequently, gold doping effectively alters the electronic properties of Graphene, rendering it semi-metallic. These findings contribute significantly to the fields of materials science and electronic applications.

## Keywords

Graphene, Gold, Ab-initio, Electronic Properties, Structural Properties, Gold Doped Graphene, Density Functional Theory

## 1. Introduction

### 1.1. Background of the Study

In the crust of the planet, carbon is one of the elements that are most prevalent. Carbon is positioned above the semiconducting elements silicon and germanium in the periodic table. It comes in a variety of forms, and every one of them has shown to be beneficial to humanity. Graphene is among these several forms. It's a carbon sheet that is hybridized with  $sp^2$ . It is a sheet of hexagonally organized  $sp^2$ -bonded carbon atoms

that is one atom thick. The purest known form of Graphene is monolayer (single layer), which has applications in high-frequency circuits [7].

A two-dimensional honeycomb lattice composed of tightly packed carbon atoms, Graphene is a monolayer that exhibits remarkable characteristics such as high conductivity and high electron mobility, measuring around  $100,000 \text{ cm}^2 \text{ V}^{-1} \text{ s}^{-1}$  at ambient temperature [22]. Conversely, Graphene is very suitable for flexible electronics and wearable devices due to its increased mechanical strength, elasticity, and stiffness. 90%

\*Corresponding author: [ttmakisa@gmail.com](mailto:ttmakisa@gmail.com) (Nigatu Desalegn)

**Received:** 31 August 2024; **Accepted:** 7 December 2024; **Published:** 17 January 2025



Copyright: © The Author(s), 2025. Published by Science Publishing Group. This is an **Open Access** article, distributed under the terms of the Creative Commons Attribution 4.0 License (<http://creativecommons.org/licenses/by/4.0/>), which permits unrestricted use, distribution and reproduction in any medium, provided the original work is properly cited.

transmittance is a very high value, primarily due to graphene's sheet resistance. The building block of graphene is fullerene, graphite, and nanotubes [20]. At 1.42 Å for the C-C bond length and 2.46 Å for the lattice parameter, the unit has two lattice sites.

First-principles calculations and tight-binding modeling (J. Slonczewski and P. Weiss, 1958) show that the valence and conduction bands intersect in a single point at the Fermi level ( $E_f$ ) (Dirac point), giving rise to a zero-gap semiconducting nature. At the Dirac point the density of states (DOS) approaches zero and the linear dispersion relation results in zero effective mass. Electrons in graphene thus behave as massless Dirac fermions. The material is expected to be useful particularly for electronic device applications, transistors.

From the early 1900s, scientists have been working with graphene; however, stable graphene structures have not been obtained in experiments until 2004. The successful preparation of intrinsic graphene has led to a booming period of research on two-dimensional materials [11]. Following this, the hot spot for basic science and advanced technology research has shifted to unique two-dimensional materials represented by graphene. Graphene has excellent properties in terms of light and electricity, force, and heat [9]. It also has excellent mechanical properties in the field of mechanics, such as Young's modulus, shear elasticity, and tensile strength, so its application prospects are very bright [12]. Graphene has been exfoliated from graphite. Graphene layer is one of the most prominent nanoscale materials currently studied; it was first studied theoretically as a textbook example for calculations in solid state physics and was discovered realistically by the Geim group at the University of Manchester, UK, in 2004. Andre Geim and Konstantin Novoselov were awarded the Nobel Prize in Physics in 2010 for this discovery. Previously, Smalley and co-workers had discovered fullerenes and Iijima had discovered nanotubes [3], which in principle are graphene sheets rolled up into cylinders and spheres. These days' carbon-based nanostructures are important for a wide range of electronic device applications [19]. One of the most well-known Nano scale materials being researched at the moment is graphene. In 1947, conducted theoretical research on graphene as a textbook example for solid state physics calculations. The Geim group at the University of Manchester, UK, made a realistic discovery of graphene in 2004. The Nobel Prize in Physics was given to Andre Geim and Konstantin Novoselov in 2010. Additionally, graphene can be employed as a transparent conductive film material in solar cells and light-emitting devices due to its exceptional conductivity, flexibility, and optical transparency. The graphene light modulator has a powerful signal transmission capacity and can send a lot of data in a short period of time (S. Iijima, 1991). Optimizing the electronic characteristics and creating nano electronic devices require a thorough understanding of the microscopic interaction between metal atoms and graphene, as the metal structures affect the charge transfer between metal and graphene [1-6]. Since the Geim group suc-

cessfully created single impurity doping in 2004 at the University of Manchester in the United Kingdom using micro-mechanical cleavage of graphite, it has garnered a lot of attention because of its intriguing characteristics and several possible uses.

Gold is a special element with features that are valuable for various sectors, such as chemical inertness, high electrical conductivity, plasticity, etc., in addition to its limited but still adequate availability (ideal for monetary applications [20]. Because of these advantageous qualities, ancient civilizations were already aware that gold was a stable, inert noble metal. As stated in reference, gold does not experience oxidation processes or lose its glossy sheen. However, in the Nano scale, gold particles smaller than 800 nm exhibit a variety of optical, magnetic, and chemical properties, radically changing their characteristics [24]. These factors make Au Nano clusters extremely promising for a wide range of nanotechnology applications, including DNA supports, light energy conversions, biosensings, and single-electron transistors. Due to the relativistic stabilization of its outer 6s orbital, gold is regarded as the noblest metal of all. Gold (Au) shows significant covalent bonding characteristics in contrast to its lighter congeners and a remarkable repertoire of chemistry, which are increasingly being utilized in catalysis and nanotechnology. These characteristics are achieved even though the relativistic effects destabilize the 5d orbital's, reducing the 6s-5d energy gap and enhancing s-d hybridization. It is desirable to investigate the doping properties and interactions between Au and graphene since there is still much to learn about the electronic properties and interactions in the Au-graphene systems.

Field effect transistors and other electronic devices can effectively use atomic doping to open the band gap of graphene. Consequently, the use of graphene in the field of field effect tubes can be enhanced by atomic doping. Based on density functional theory, doping atoms to alter Graphene's electrical characteristics offers some fundamental theoretical support for the material's advancement and strengthens its influence in band gap engineering applications, which include sensors, new energy batteries, Nano electronics, super capacitors, and other devices [23]. According to additional research, the material's Dirac point changes as the number of doped atoms grows and it exhibits more significant p-type semiconductor characteristics. It is anticipated that the material will be especially helpful for transistor applications in electronic devices. Because of its intriguing qualities and wide range of possible uses, it has garnered a lot of attention. The goal of the current work is to examine how doping affects Graphene's electrical and structural characteristics and how these change with sheet size [17].

DFT Foundations Kohn-Sham equation, a single particle independent Schrodinger equation, can be derived from the Schrodinger equation for a multi body system and solved numerically using density functional theory. Scientist Walter Kohn won the 1998 Nobel Prize for his work on wave functions, which is the basis for this theory that determines the

physical properties of solids by computation. Total density, as stated by Thomas and Fermi in 1927, is the crucial quantity in many body problems, even if at the time no exchange-correlation effects had been observed. The framework for DFT was established in 1964 by the theorems of Hohenberg, Kohn, and Sham, which stated that all properties in the absence of a magnetic field could be fully characterized by the (non-degenerated) ground state electron charge density of a many-body problem [13]. It is generally assumed that one type of substrate implies a specific type and level of doping, even though specific DFT calculations can produce different results for the same metal. Any discrepancies are thought to be related to the limitations of ab methods, the outcomes of which depend on the calculation strategy and the choice of exchange-correlation interaction. Consequently, the current investigation focuses on the electrical and structural characteristics of gold-doped graphene, expanding the range and potential applications of graphene materials. In addition to strengthening graphene's influence on band gap engineering applications—such as those in sensors, new energy batteries, nano electronic devices, super capacitors, and other devices—it offers some fundamental theoretical contributions to the material's advancement.

## 1.2. Statement of the Problem

Recent years have seen a huge increase in interest in graphene, one of the most significant two-dimensional (2D) materials, due to its excellent properties, including high current carrying capacity, carrier mobility, Klein tunneling, saturation velocity, am bipolar effect, unique quantum hall effect, thermal conductivity, and non-zero Berry's phase [9]. These properties have led to a wider range of applications in catalysts, interconnects, transparent electrodes, radio frequency transistors, and sensors. However, a major barrier to the widespread application of conventional optoelectronic fields is Graphene's lack of an electronic band gap. In order to meet the requirements for practical applications, a great deal of effort has been made to open the band gap of graphene [8]. In recent years, researchers have found that doping graphene with heteroatoms can open up its band gaps and significantly alter its electronic effects so studying the properties of graphene by adding different atoms has become a hot topic. In their investigation of graphene combined with various nitrogen atom concentrations, they found that pure graphene and commercial carbon black XC-72 had higher catalytic activity in the cathode oxygen reduction reaction of fuel cells. Examined the performance of intrinsic and doped graphene systems and noted that doping P and S would significantly improve the capacitive performance of the ultra-capacitor in graphene. Density functional theory was used to investigate the adsorption of graphene doped with boron, nitrogen, aluminum, and sulfur. In their study of Li doped graphene, they observed that doped lithium columnar oxide graphene has the ability to store hydrogen, a nanomaterial, and provided a

scientific explanation for the cross-sectional energy conversion and storage. After examining the structure, electrons, and magnetism of graphene doped with tungsten atoms proposed that magnetism is significantly influenced by the spacing of tungsten atoms. According to research on graphene oxide by [11-14], graphene, highly reduced graphene oxide, and graphene can all be employed as multifunctional building blocks in carbon-based materials. Carbon nanosheets, on the other hand, can be used as fillers in polymers and inorganic nanocomposites as well as sole components in paper and film. Consequently, it is evident that doped and intrinsic graphene systems have research and practical applications in common. Graphene has been investigated with various doping, but these are not adequate for all uses, thus researchers are still looking for better ways to employ graphene in more fields. Graphene must have its characteristics altered by various doping in order to function better. Further research is necessary to fully understand the various unique features of Au doping in graphene, as it is currently understood to be incomplete. Furthermore, graphene structure is inexpensive to produce and conveniently accessible. In the last few years, computer modeling has advanced our understanding of graphene. Further work is required to fully comprehend this material's special qualities. Hopefully, graphene will find additional uses in nanotechnology if these problems are solved. In order to provide graphene with great properties and contribute to the advancement of science and technology in the future, this study will analyze and compare the effects of doping with Au on the electron density, state density, and energy band of graphene.

## 1.3. Objectives of the Study

### *General objective of the study*

The general objective of this study was to determine the electronic and structural properties of gold doped graphene.

### *Specific objectives*

The Specific objectives of this study were:

- 1) To find the kinetics energy cut-offs for the plane wave expansion of the wave functions;
- 2) Determine the structural properties of the systems such as the equilibrium lattice constant;
- 3) To determine the effect of gold on graphene;
- 4) Determining the DOS of both pristine and gold-doped graphene;
- 5) Examining the band structure of both pristine and gold-doped graphene;

## 1.4. Significance of the Study

It is astounding how much we have discovered about the two-dimensional physical properties of materials in the nearly two decades since the production of graphene. Nonetheless, there is a growing body of research on so-called nanomaterial, both in terms of discovering new

chemicals and using Nano manipulation to modify their structural and electrical characteristics. This race has a very apparent justification: 2D materials open up a limitless number of new fundamental scientific phenomena and technology applications. Because of these characteristics, graphene is a suitable material for a wide range of applications in nanocomposites, energy research, quantum physics, catalysis, nanoelectronics, biomaterials, and nanomedicines. These applications include drug delivery platforms for tissue engineering and cell culture, bioimaging, biosensings, gene therapy, and antibacterial applications. Consequently, by using quantum espresso to explore the properties of graphene by adding gold doped graphene, we have established a foundation for nano-related research and innovations based on computational techniques, and we are a good support for empirical studies in the future. It's also helpful to remember that quantum espresso is a freely available package and that the method is an economical one. Furthermore, it might serve as a resource for scholars to carry out additional research in the field.

### 1.5. Scope of the Study

The entire minimum energy of gold-doped graphene per atom, total stress, and equilibrium lattice constant with respect to various parameters such as energy cut-off, k-point sampling, degauss, and smearing for k-point sampling are the only calculations that fall under the purview of this study. The research would also be restricted to examining the electrical and structural characteristics of the material, which is gold-doped graphene. The study's methodology would be limited to theoretical and computational aspects.

## 2. Review of Literature

The electrical and structural characteristics of molecules, cells, or bulk materials can be studied using DFT. Using the ideas of quantum physics, the DFT offers a framework for obtaining the electronic, structural, and total energy. A wide range of systems and issues in physics, chemistry, biology, and material science can also be solved with DFT. The Schrödinger equation addresses every issue pertaining to the electrical structure of matter, including time. But most of the time, one is interested in molecules and cells that do not interact over time, thus we may concentrate on the time-independent Schrödinger equation [12-19]. With merely the constituents' cell numbers as an input, the Schrödinger equation may be solved to determine energies and forces, which should accurately reflect the bonding between the cells. Since it is impossible to solve the Schrödinger equation for the complicated many-cell, many-electron system analytically, numerical methods have proven to be quite helpful in the fields of physics, chemistry, and materials research.

### 2.1. Structural Properties of Graphene/Hexagonal Heterostructures

Structurally graphene is a single layer of 2D atomic crystals with a hexagonal lattice structure. Theoretical investigations indicated that bond length, thickness of the layer and inter-layer distance of isolated Graphene is around  $1.43\text{\AA}$ , as shown Figure 1. Reported experimental Values are C-C  $1.42\text{\AA}$ . And, also by  $sp^2$  orbital hybridization, causing occupied and un-occupied states to move away from each other [21].

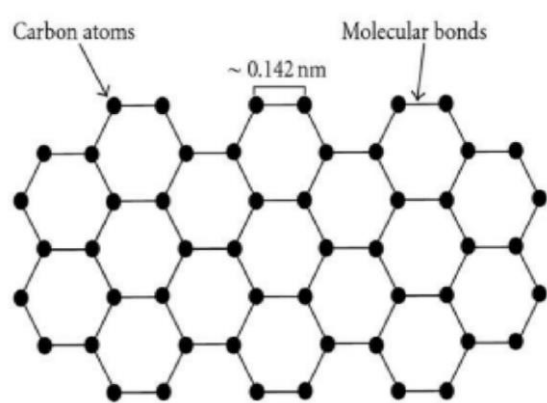


Figure 1. Schematic structure of graphene sheet.

The conduction and valence bands of graphene, a zero-band-gap semimetal with six extremely symmetrical K points in the Brillouin zone, intersect at the Dirac point. Gradually, the substrate is recognized as a technique for expanding the graphene band gap. It is possible to use carbon as a substrate to widen the band gap of graphene since it is an conductor material with a band gap of  $5.97\text{eV}$ , has an atomically flat surface, very low roughness, no dangling bonds on its surface, and similar lattice structure to graphene due to lattice mismatch about  $1.84\%$ . This is due to the gravitational interaction between electrons of graphene monolayer. Electronic properties of G can be obviously modified by 3d TM doping. By doping Gold (Au) on the lateral structure of G displays that the electronic properties behave like a spin-polarized half semiconductor with direct band gap of  $0.27\text{eV}$  for majority spin channels and indirect gap  $0.32\text{eV}$  for minority spin channels [23].

### 2.2. The Hexagonal Structure of Graphene in Two Dimensions

A flat monolayer of carbon atoms densely packed into a two-dimensional (2D) honeycomb lattice is known as graphene, and it serves as the fundamental building block for all other graphitic materials (Figure 1). It can be rolled into 1D nanotube, stacked into 3D graphite, or wrapped into 0D fullerenes. Theoretically, features of many carbon-based materials can be described by graphene, also known as "2D



graphite," which has been studied extensively for sixty years. Two-dimensional graphene, or graphene, is a semiconductor with zero gaps. Graphene's strong two-dimensional structure makes it a promising material for modern uses. A sheet of  $sp^2$ -carbon atoms firmly packed into a two-dimensional honeycomb lattice, one atom thick, is known as single-layer graphene. All graphitic forms of carbon, such as three-dimensional graphite, one-dimensional carbon nanotubes, and zero-dimensional fullerenes, are descended from it. To observe the influence on its structural and electrical properties, different elements are either adsorbed on the graphene sheet at different places or doped onto it [17].

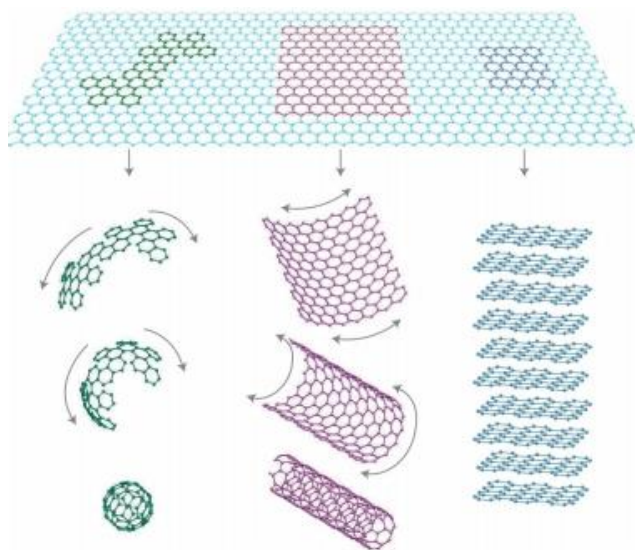


**Figure 2.** Graphene (2D) is the main component of carbon materials with different morphologies.

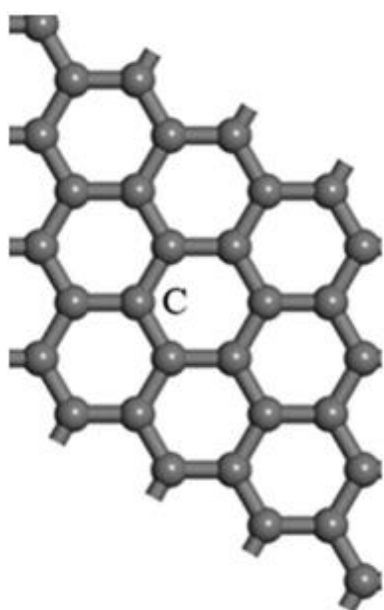


**Figure 3.** Intrinsic graphene model ( $4 \times 4 \times 1$ ).

The graphene simulation model that is being used is a model-optimizing graphene model. Graphene has the chemical formula C. Its single-layer atomic ring structure is stable and symmetrical, with hexagonal structural characteristics. Each C atom forms a solid chemical link with three other neighboring C atoms to form a covalent molecule, which also forms a molecular structure. In order to improve the accuracy of the computation outputs, a bigger scale system must be built after the metacell is completed. Taking into account that the computational volume of the system grows geometrically as it climbs up, the  $4 \times 4 \times 1$  supercell model is constructed to represent graphene, and is illustrated in detail in Figure 3.

Graphene's distinct chemical structure and shape give it remarkable properties. These characteristics include: high charge mobility ( $2 \times 10^5$  cm<sup>2</sup>/Vs., 200 times greater than silicon), electron transport capability, enormous specific surface area (2630 m<sup>2</sup>/g), high electrochemical activity with high chemical stability, high specific capacity (theoretical value of 744 mAh/g) and specific capacitance (550 F/g), ultra-high surface to volume ratio, an ultrahigh Young's modulus of almost 1.1 TPa, intrinsic fracture strength of 125 GPa, and good biocompatibility are a few of these properties. The primary mechanical, electrical, chemical, and physical properties of graphene-based materials are covered in this section from a variety of angles. Because of its minuscule band gap, graphene is more significant in the electronics industry. Even though graphene synthesis is a laborious process, creating huge amounts of it for commercial uses will lower costs and make the material easier to produce. The highest occupied band of a metal at 0K has some electrons in it. At zero degrees Celsius, all of the electrons in a semiconductor are fully occupied in the highest band and all of the remaining bands are unoccupied. The band gap  $E_g$  is the distance between the two bands. A permitted band's electrons are unable to conduct any current when they are fully packed with electrons. Since an electron can only go into an empty state, being fermions prevents them from carrying any net current in a filled band. This phenomenon means that a material with a totally filled band and an empty, energy-separated next permissible band can theoretically have infinite resistivity and function as an insulator or semiconductor. A metal is a substance whose band of electrons is only half filled. It has an extremely low resistance. In semiconductors, the upper empty band is referred to as the conduction band, while the band that is typically filled with electrons at 0K is known as the valence band. With doping or applied electric potentials, semiconductors' conductivity can be changed by orders of magnitude. Semiconductors have zero conductivity at 0K and relatively poor conductivity at limited temperatures. Semiconductors are hence advantageous for active devices [9].

The 2D planar sheets that make up prime Graphene are made up of virtually unbreakable covalent connections between  $sp^2$  carbons atoms organized in hexagonal patterns. Graphene exhibits non-linear elastic properties in addition to

being rather brittle. The equation  $\sigma = E_e + D\epsilon^2$  describes the nonlinear elasticity under a tensile load. Here,  $\sigma$  represents the applied stress (second Piola Kirchhoff),  $E$  stands for Young's modulus,  $\epsilon$  is the elastic stress-strain (uniaxial Lagrangian), and  $D$  is the experimentally determined constant of third-order elastic, where  $E = 1.0$  TPa and  $D = 2.0$  TPa (Fatemeh Farjadian, 2020). When a critical stress (about 130 GPa) is applied in accordance with the material's intrinsic strength, a brittle fracture results. Because of the high values of  $E$  and  $\sigma_{int}$ , Graphene is regarded as an extremely durable material for structural uses. Moreover, grapheme's elasticity is another advantageous characteristic. Graphene oxide paper has average fracture strength of 80 MPa and an average elastic modulus of 32 GPa [10].

Grapheme's intrinsic strength is another one of its remarkable qualities. Because of the strength of its carbon bonds, Graphene possesses the highest tensile strength of any material yet discovered— $13 \times 10^{10}$  Pascal's, or 130 GigaPascals—compared to  $4 \times 10^8$  for steel, or 200 times stronger. Graphene is not only extraordinarily strong, it is also the lightest material, even though it is lighter than paper. It is 0.77 milligrams per square meter (for comparison purposes, 1 square meter of paper is roughly 1000 times heavier). Graphene also contains elastic properties; it is able to take its initial size after strain. It is often said that a single sheet of graphene is sufficient enough in size to cover a whole football field, and would weigh less than 1 single gram. In 2007, Atomic force microscopic (AFM) tests were carried out on graphene sheets that were kept out over silicone dioxide cavities. These tests showed that graphene sheets had spring constants in the region of 1 -5 N/m and a Young's modulus of 0.5 TPa which is different to that of three-dimensional graphite.



**Figure 4.** Show that it takes an elephant balanced pencil to pierce a sheet of graphene, (b) flexibility of graphene transistor.

Free  $\pi$  electrons, which make up the graphene structure, can engage through electrophonic interactions with the frontier molecular orbitals (FMO) of other nearby organic molecules. Additionally, the planar structure permits a number of reactions, including carbene insertion; click reactions, and cycloaddition, which converts  $sp^2$  hybridization into  $sp^3$  hybridization. Topological defects such heptagons, pentagons,

and their combinations, adsorbed impurities, edges, vacancies, and fissures can therefore be produced by these reactions. In geometrically stressed places, like edges, whether they have zigzag or arm-chair formats, the aromatic rings are more reactive; in fact, zigzag edges are more reactive than arm-chair edges. [14].

Graphene is a zero-overlap semimetal. In Graphene each carbon atom is connected to three other carbon atoms. It has 6 carbon electrons, with four electrons in  $n$  shell (outer shell). These four electrons of each carbon atom when bonded with other three carbon atoms having the same number of outer shell electrons leave 1 electron freely available. This freely available electron causes conduction to take place. These electrons are commonly known as  $\pi$ -electrons. These are located in between two graphene ultra-thin layers. Thus these  $\pi$ -electrons cause overlapping of  $\pi$ -orbital making the carbon-carbon bond in graphene much stronger. From the chemistry point of view, one can say that carbon atoms in graphene are connected to each other covalently by three  $\sigma$  bonds in plane and the remaining out of plane  $\pi$  orbital would contribute in delocalized electrons' network. It is noteworthy to mention that, from scanning electron microscopy (SEM) investigations it has been proved that graphene has zigzag and armchair-like crystal edges, the chemistry behind this phenomenon would be worthy of investigation. Owing to the  $\pi$ - $\pi$  stacking its surface may interact easily with many other molecules, and the surface can be activated to a greater extent as a result of chemical functionalization [11].

The electrical capabilities of graphene have garnered greater attention than its other remarkable characteristics. One can classify graphene as an intrinsic semiconductor due to its unique Fermi energy level configuration and linear Dirac-like spectrum. Double-layer Graphene's band overlap has a very tiny and insignificant parabolic spectrum of 1.6 meV. As such, it can be seen as a substance that resembles metal and incorporates a single kind of exaction. It should be noted that the band structures of graphene with three or more layers are complex, containing many charge carriers that overlap the valence and conduction bands. On a non-conductive substrate, Graphene's charge mobility is around  $1.5 \times 10^4$   $\text{cm}^2/\text{Vs}$ . at 300 K and  $6 \times 10^4$   $\text{cm}^2/\text{Vs}$ . at 4 K, respectively, with a maximum concentration of  $10^{13}$   $\text{cm}^2$  of electrons and holes. Because of Graphene's exceptional conductivity, its sheet resistance (RS) is incredibly low—30  $\Omega/\text{sq. cm}^2$ . [17-20]

The fact that graphene is a semimetal with both electrons and holes acting as charge carriers and has a high electrical conductivity is one of its most significant characteristics. Each carbon atom in graphene is joined to three other carbon atoms in a two-dimensional plane; yet, a carbon atoms electrical arrangement indicates that it possesses six electrons total—two in its inner shell and four in its outermost shell. Because these four outer shell electrons participate in chemical bonding, one electron from each carbon atom is available for electronic conduction in the third dimension in graphene. The extremely mobile electrons above and below the gra-

phene sheet are known as  $\pi$  ( $\pi$ ) electrons. The carbon to carbon bonds in Graphene are strengthened by the overlap of these  $\pi$  orbitals. Essentially, the bonding and ant bonding (valence and conduction bands) of this  $\pi$  orbital control grapheme's electrical characteristics. The c-c bonds in Graphene are strengthened by these electrons. [22] Because of its many uses, graphite and its derivatives have recently attracted the attention of scientists and engineers. In the realm of material science, Graphene's discovery is rightfully considered a turning point, as seen by the widespread interest the material has garnered in the domains of electronics, photonics, capacitors and super-capacitors, biosensings, etc. Photo catalysis, electronics, gas sensing, graphene-based heterogeneous electrodes for energy storage devices, and other fields are some of these applications. Furthermore, audio devices Graphene-based radio wave absorption A layer of heaven-crammed graphene placed on glass substrates absorbs 90% of radio waves in the 125–165 GHz frequency range.

#### 1) Energy Holding

Energy storage is one topic of research that is receiving a lot of attention. The last several decades have seen rapid advancements in all areas of electronics (Moore's law states that the number of transistors employed in electronic circuitry doubles every two years). However, there is always an issue with batteries and capacitors that store energy when it is not in use. The issue is that while a battery has the capacity to store a large amount of energy, charging a capacitor is faster but results in a smaller amount of energy being stored than with a battery. The answer to energy storage is to create a component that can both store and charge energy rapidly, like a super capacitor or battery. Because of grapheme's excellent electrical conductivity, super capacitors—which can store a lot of electricity and charge quickly—have been built using Graphene? Scientists are actively using Graphene as an anode in lithium ion batteries to improve their performance and provide significantly bigger storage capacity with improved charge rates. Laptops and smartphones, among other devices, employ lithium ion batteries [16].

#### 2) Application in biomedicine

Graphene has many beneficial uses in the biomed field. Important uses of graphene in biomedicine include graphene-based biosensors for tiny molecules (like glucose), graphene-based bio imaging, and PTT (photo thermal treatment). PTT is a therapy that uses the structural design of nanomaterial's to limit tumor growth. Graphene-based Nano-materials are viable cancer treatment vehicles due to the special physical and chemical features of graphene, including its ability to absorb infrared light [7].

#### 3) Plasmonics

The study of Plasmonics has recently found that infrared spectroscopy of Graphene and near field infrared optical microscopy provides accommodations for Plasmonics surface mode. Plasmonics lasers, specifically Nano scale Plasmonics nanowire lasers; have been the subject of extensive research due to their unusual properties, particularly with regard to

their ability to operate above the traditional diffraction limit. I-VI semiconductor nanowire, which has a high optical gain, can be combined with a metallic nanostructure to achieve Plasmonics lasing oscillation. For ten years, single-cell activity analysis has utilized Plasmonics imaging. More work needs to be done to increase Plasmonics imaging's imaging capabilities. The spatial resolution of SPRM is severely limited in the direction of the Plasmonics waves because of the propagation of Plasmonics waves on the sensing chips, generating interference fringes with lengths of several micrometers.

#### 4) Absorption of radio waves

A layer of perfectly packed graphene placed on glass substrates absorbs 90% of radio waves in the 125–165 GHz frequency range. Graphene is used as window, door, and roof coatings in modern homes to protect them from radio wave interference.

#### 5) Tiny antennas

Within the radio frequency range, Nano antennas known as Graphene-based Plasmonics Nano antennas (GPN) function at a millimeter wavelength. Because of its significantly lower operating surface Plasmon polarities wavelength than the wavelength of electromagnetic waves propagating at the same frequency, this Nano antennas performs better than our conventional antennas. In comparison to GPNs, our traditional antennas operate in the enormous range of 100 to 1000 frequencies [2].

## 2.3. Doped Graphene's Properties

Atomic doping offers an efficient means of opening Grapheme's band gap for electronic devices like field effect transistors. As a result, atomic doping can improve the way graphene is used in field effect tubes. P-type and n-type FETs are the two different types of FETs. Positively charged holes predominate in p-type semiconductors, which are used in p-type field-effect tubes Because of its outer 6s orbital stabilization by relativistic means, gold is considered the noblest metal. While the relativistic effects cause the 5d orbital's to become unstable, thereby decreasing the 6s–5d energy gap and improving s–d hybridization, Gold (Au) shows notable covalent bonding characteristics in contrast to its lighter congeners and a remarkable chemistry repertoire that is being used more and more in catalysis and nanotechnology. It is desirable to investigate the doping properties and interactions between Au and graphene since the electronic properties and interactions in the Au–graphene systems are not well understood at this time [23].

One of the highest specific surface areas is found in 2D materials, particularly graphene, which is necessary for a high adsorption capacity. Early studies on gold-doped graphene demonstrated that, through a redox interaction between graphene and gold ions, graphene could chemically convert aqueous gold ions to metallic gold. These two characteristics taken together imply that graphene might be a promising



option for the extraction of gold. Graphene's enormous surface area is scarified and its dispensability in aqueous gold solution is poor due to its inherent hydrophobicity, which may be the reason for the absence of successful graphene extraction experiments..

The Gold nanoparticles are colloids that have been known since ancient times for their fascinating properties and coolers. Why is there such great current interest in gold nanoparticles (AuNPs). Because of, Facile methods of synthesis and Stability in a wide variety of solvents, High degree of control over size and shape and Wide range of medical and industrial applications. And, it is the most malleable and ductile metal, it is frequently alloyed to increase strength and endurance. While gold has a high reflectivity for red and infrared wavelengths, it has a poor reflectivity for ultraviolet and visible light rays. Due to its ease of reshaping and long-lasting brightness, gold has long been utilized in dentistry, medical, electronics, computers, medals, and prizes, as well as jewelry and decoration. But because of its superior conduction qualities and resistance to oxidation-induced corrosion, gold is also used in electronics nowadays. The atomic 6s states delocalize over the cluster atoms in the case of gold, forming a super atom with a shell structure. For instance, cluster size affects gold's electron affinity. But gold clusters also have unique characteristics that set them apart from other metal clusters. For instance, because Au is a heavy metal with a large nuclear charge, relativistic effects are important due to the high kinetic energy of its core electrons. Six-s valence orbital constrict as a result of these actions, whereas five-d valence orbital expands-d hybridized states result from a reduction in the energy gap between the s and d states. These states play a critical role in the bonding of Au atoms, and the bonds are strongly directed due to the d nature. However, the finding that gold is catalytically active in cluster form even though it is an inert noble metal in bulk form has likely been the primary driver of the recent research gold rush over the past 20 years. In fact, gold is the best catalyst for the acetylene hydro chlorination reaction on a carbon support, in addition to being a catalyst [21-24]. The general properties of solid that of the highest occupied band of a metal at 0K has some electrons in it. At zero degrees Celsius, all of the electrons in a semiconductor are fully occupied in the highest band and all of the remaining bands are unoccupied. The band gap  $E_g$  is the distance between the two bands. A permitted band's electrons are unable to conduct any current when they are fully packed with electrons. Since an electron can only go into an empty state, being fermions prevents them from carrying any net current in a filled band. This phenomenon means that a material has unlimited resistivity and can be either an insulator or a semiconductor when one of its bands is fully occupied and the next permitted band is vacant and separated in energy. A metal is a substance whose band of electrons is only half filled. It has an extremely low resistance. In semiconductors, the higher, empty band is referred to as the conduction band, and the band that is typically filled with electrons at 0 K is known as the

valence band. With doping or applied electric potentials, semiconductors' conductivity can be changed by orders of magnitude. Semiconductors have zero conductivity at 0K and relatively poor conductivity at limited temperatures. Semiconductors are hence advantageous for active devices [12].

## 2.4. Schrödinger's Equation

Electrons and celiac nuclei make up all materials. The location of these electrons and ions is the only factor influencing the macroscopic characteristics of the substance that we see. Therefore, the (time independent) Schrödinger equation may be used to determine the wave function and energy of the system with just the type of cells and the material that it is composed of. Given by is the stationary Schrodinger equation.

$$H \Psi = E \Psi \quad (1)$$

Where E is the system's total energy and H is the Hamiltonian. The total wave function, which in theory incorporates all desired system features and is therefore crucial to quantum mechanics, is obtained by solving this equation. Finding this wave function, or equivalently, as in the case of DFT, the density  $n(r) = |\Psi|^2$ , is the aim. The Hamiltonian for the many-body problem of a system with K nuclei and N electrons and charge ZI was computed as [3-5].

$$H = -\sum_{i=1}^N \frac{\hbar^2 \nabla_i^2}{2m_e} - \sum_{i=1}^M \frac{\hbar^2 \nabla_i^2}{2M_n} - \sum_{i=1}^M \sum_{j=1}^N \frac{Z_i e^2}{|r_i - r_j|} + \frac{1}{2} \sum_{i=1}^N \sum_{j>1}^N \frac{e^2}{|r_i - r_j|} + \frac{1}{2} \sum_{i=1}^M \sum_{j>i}^M \frac{Z_i Z_j e^2}{|r_i - r_j|} \quad (2)$$

With: - N: number of electrons

$r_i$ : electronic coordinate

M: number of nucleus atom

$r_j$ : nuclear coordinate

$M_n$ : mass of the nucleus

$Z_i$ : atomic number of the nucleus

$m_e$ : mass of electron

The electron and nucleon kinetic energies,  $T_e$  and  $T_n$ , are represented by the first two terms. The electrostatic repulsion between the electrons is represented by the third term,  $V_{ee}$ . The electrostatic attraction between the nuclei, represented by  $V_{nn}$ , and the electrons, represented by  $V_{ne}$ , is the fourth term. The mass of the cores is MI, while the mass of the electrons is me. Each core has a certain number of protons, ZI. This appears to be a somewhat intricate task. It turns out that only a one-electron system, such as the hydrogen cell or the ionized helium cell He+, can have the stationary Schrödinger's equation analytically solved. Thus, some approximations must be made in order to proceed. The Born-Oppenheimer approximation is typically used as a first approximation and is justified by the fact that the nuclei (ions) are substantially heavier than the electrons,  $MI \gg me$ . This often argues that a time-scale gap is justified by the electrons' quick adaptation to ion location changes. This implies that the electronic and ionic



systems can be handled independently, with the ions being thought of as fixed for the electrons. Consequently, we may exclude the parts in the Hamiltonian that deal with ionic kinetic energy and ion-ion interaction, leaving just the terms that deal with electrons.

$$H_{BO} = -\sum_{i=1}^N \frac{\hbar^2 \nabla_i^2}{2m_e} - \sum_{i=1}^M \sum_{j=1}^N \frac{Z_i e^2}{|r_i - r_j|} + \frac{1}{2} \sum_{i=1}^N \sum_{j>1}^N \frac{e^2}{|r_i - r_j|} \quad (3)$$

If we denote the interaction of electron  $i$  with the ions  $V_{ext}(r_i)$  and use Hartree celiac

Units  $\hbar = m_e = e = \frac{1}{4\pi\epsilon_0} = 1$ , we can write the Hamiltonian as

$$H = -\frac{1}{2} \sum_i \nabla_i^2 + \sum_i \sum_j \frac{1}{|r_i - r_j|} + \sum_i V_{ext}(r_i) \quad (4)$$

The Hamiltonian  $H(t) = T + V(t) + W$  is assumed to consist of the kinetic energy, spin-independent single-particle potential and some spin-independent particle-particle interaction.

## 2.5. Density Functional Theory

The model of choice for comprehending condensed matter at low energies is density functional theory, or DFT. It has established itself as a common first-principles technique. Yes, for a great deal of important condensed-matter phenomena, but not all of them. Among other things, electrical, vibrational, magnetic, and superconducting phenomena can all be studied effectively with DFT. A quantum mechanical method called density functional theory (DFT) is utilized in chemistry and physics to study the electrical and structural characteristics of various body systems. DFT has shown to be incredibly effective at characterizing the structural and electrical characteristics of a wide range of materials, from molecules and cells to basic crystals and intricate extended systems (which include gases and liquids) (M.P. Das and F. Green, 2016) [21]. DFT also has relatively simple computational requirements. Due to these factors, DFT is now often used in first-principles simulations meant to characterize or even forecast the characteristics of condensed matter and molecular systems (C. Fiolhais, 2003) (R. G. Parr, 1989). Conventional approaches in electronic structure theory rely on the complex many-electron wave function, notably Hart-tree-Fock theory and its offspring. Density functional theory aims to substitute the electronic density as the foundation quantity for the many-body electronic wave function. The density is merely a function of three variables and is a simpler quantity to deal with both conceptually and practically than the many-body wave function, which is reliant on  $3N$  variables, three spatial variables for each of the  $N$  electrons. With the publication of their two key theorems in 1964, Hohenberg and Kohn laid the groundwork for DFT. The introduction of the significant DFT development milestone by Hohenberg, Kohn, and Sham (HKS) occurred in 1965. They demonstrated that DFT was an exact theory in the same sense as the wave function theory in

order to provide proofs for these propositions.

## 2.6. The Hohenberg-Kohn Theorems

The two theorems that underpin the Hohenberg-Kohn formalism [4] of DFT are:

### The First Theorem

The ground state particle density,  $n_0(r)$ , determines the potential  $V_{ext}(r)$  uniquely, up to a constant, for any system of interacting particles in an external potential  $V_{ext}(r)$ .

### The Second Theorem

The energy functional for the system is defined by the second HK theorem, which also establishes that the energy functional is minimized by the appropriate ground state electron density. The density  $E[n]$ 's energy functional is as follows:

$$E[n] = \int dr V_{ext}(r) n(r) + F[n] \quad (5)$$

Where, the kinetic and potential energy are included in  $F[n]$ , a universal functional of the density. The ground state energy  $E_0$  of the energy functional  $E[n]$  is located at the physical ground state density  $n_0(r)$  once the external potential  $V_{ext}(r)$  has been fixed.

$$E_0 = E[n_0] \quad (6)$$

The Hohenberg-Kohn (HK) theorems do not deduce the exact expression of the universal functional of the electron density; rather, their restricted objective is to demonstrate that such a functional exists. Because, with the exception of basic metals, there is no well-known equation for the kinetic energy as a functional of  $n$ , a direct minimization of the functional is typically not applicable. Most of the actual calculations begin with the Kohn-Sham (KS) scheme, which is a reformulation of the theory based on the KS orbital's instead of the mere density.

## 2.7. Kohn-Sham Equation

By solving a single particle-like equation, the Density Functional Theory (DFT) in the Kohn-Sham formalism offers a potent computational technique that makes it possible to precisely estimate the ground-state properties even of complicated systems for interacting particles. For self-consistent field electronic structure calculations of the ground state characteristics of cells, molecules, and solids, Kohn-Sham density theory is frequently utilized. The equation of Kohn and Sham as:

$$\left[ \frac{1}{2} \nabla^2 + V(r) + V_H(r) + V_{xc}(r) \right] \psi_i(r) = \epsilon_i \psi_i(r) \quad (7)$$

Where  $V_{ex}(r)$  is the external potential, and  $\psi_i$  is the Eigen function. The intractable many-body issue of interacting electrons in a static external potential is reduced to a tractable

problem of non-interacting electrons moving in an effective potential within the framework of Kohn-Sham DFT (KS DFT). The external potential plus the results of the Coulomb interactions—such as the exchange and correlation interactions—between the electrons make up the effective potential. The challenge in KS DFT is modeling the latter two interactions.

## 2.8. Exchange-correlation Energy

By decomposing the many-body problem into a collection of single-particle difficulties, the KS DFT offers a workable method for solving the problem. Although this formalism is exact, it is practically still unsolvable since the exchange-correlation term  $EXC[n]$ , whose precise form is unknown, still includes the many-body wave functions. It is required to make some estimates for the exchange-correlation term  $[n]$  in order to make the formalism useful. The Local Density Approximation (LDA) is the most widely used and simple approximation to (G. Vignale and M. Rasolt, 1987).

### A. Local-Density Approximations (LDA)

The LDA operates under the assumption that, at any given place in space, the exchange-correlation energy per electron of a non-uniform system is equal to that of a uniform electron gas with the same density at that same point. The exchange-correlation functional in LDA is expressed as

$$E_{xc}^{LDA}[n] = \int (n(r)) \varepsilon_{xc}^{hom} n(r) dr \quad (8)$$

Where, the exchange-correlation energy density is denoted by  $(\rho(r))$ . Each of the infinitesimally tiny regions (placed at locations  $r$ ) in the many-electron system has a homogenous interacting electron gas with a constant local density  $(\rho)$ . Specifically, the LDA is accurate when the density is constant, but it also performs admirably in situations that are more like reality. The local spin density approximation is used to simulate magnetic materials, splitting the electron density into spin up and spin down densities  $(\rho \uparrow(r))$ ;  $(\rho \downarrow(r))$  with  $(\rho(r)) = (\rho \uparrow(r)) + (\rho \downarrow(r))$ . The above equation can be expressed as follows by using the spin polarization:  $\zeta(r) = \rho \uparrow(r) - \rho \downarrow(r) / \rho \uparrow(r) + \rho \downarrow(r)$ .

$$E_{xc}^{LDA}[\rho(r)], \zeta(r)] = \int \rho(r) \varepsilon_{xc}^{hom} \rho(r) \zeta(r) d^3(r) \quad (9)$$

In order to develop more complex approximations to the exchange-correlation energy, such as hybrid functional approximations or generalized gradient approximations, local-density approximations are crucial. Any approximation exchange-correlation functional that reproduces exactly the results of the homogeneous electron gas (HEG) for non-varying densities is a desirable quality. LDAs are hence frequently a clear part of such functions. Since the exchange correlation energy  $[n]$  at any place in space depends only on the electron density at that same site, the LDA is by definition local. For a uniform electron gas with a range of electron

densities, the  $[n]$  has been computed and parameterized using Monte Carlo total energy calculations. LDA is only supposed to be accurate for systems necessary for the GGA function to function. One way to express this is where the electron density varies slowly because it is based on uniform electron gas. It is obviously unsuitable for environments with abrupt variations in electron density, such as covalently bonded materials.

A different type of swapped correlation functional known as the Generalized Gradient Approximation (GGA) has been developed in order to address this shortcoming of LDA. Both the local electron density and the spatial fluctuation in electron density, which is represented by the density gradient GGA functional is as

### B. Generalized Gradient Approximations (GGA)

While they are still local, generalized gradient approximations (GGA) additionally account for the density gradient at the same coordinate. The GGA frequently results in improvements to a molecule's binding energies, structural characteristics, and overall energy. Where the gradient  $|\nabla \rho(r)|$  of the electron density and its exchange-correlation functional are both dependent on:

$$E_{xc}^{GGA}[\rho(r)] = \int \rho(r) \varepsilon_{xc} \rho(r), \nabla \rho(r) d^3(r) \quad (10)$$

This is an electron gas's exchange correlation energy per particle. Though computationally more demanding than LDA the GGA calculations yield better total energies particularly for tiny molecules. In general, GGA is superior to LDA in the following ways [15]: it enhances the ground state characteristics of molecules, light cells, and clusters; it accurately predicts the magnetic properties of three-dimensional transition metals, including body-centered iron. Despite appearing to be better than LDA, GGA has a number of disadvantages. The hydrogen bond is not accurately treated by a GGA approach. The swelling and subsequent weakening of bonds is a blatant sign of this deficiency.

### Time-based system

We used lattice vectors  $a_1$ ,  $a_2$ , and  $a_3$  to define the geometry of the system, which is a periodic repetition of a cell in space. Bloch's theorem states that the solution to the Schrödinger equation for this periodic system must meet certain essential requirements.

According to Bloch's theorem, each electronic wave function in a periodic material can be expressed as the product of the wave-like and cell-periodic parts [19].

$$\psi_k(r) = e^{ik \cdot r} u_k(r) \quad (11)$$

Where is space-periodic with the super cell's periodicity. That is, for any numbers  $n_1$ ,  $n_2$ , and  $n_3$ ,  $(r + n_1 a_1 + n_2 a_2 + n_3 a_3) =$ . According to this theorem, the Schrödinger equation can be attempted to be solved independently for every value of  $k$ . using a basis set made up of a discrete set of plane waves whose wave vectors are reciprocal lattice vectors of the crystal, the cell-periodic part of the wave function can be

enlarged.

$$u_k(r) = \sum_i C_i G e^{iG \cdot r} \quad (12)$$

In this case,  $G = 2\pi n$  for all  $n$ , where  $n$  is a crystal Lattice vector and  $n$  is an integer, defines the reciprocal Lattice vectors  $G$ . Consequently, the sum of plane waves can be used to represent any electronic wave function.

$$\psi_k(r) = \sum_G C_{i,k} + G e^{i(k+G) \cdot r} \quad (13)$$

Discrete plane wave basis set is currently used to define the electrical wave functions at each  $k$ -point. This Fourier series is infinite in theory. An infinite basis set, however, cannot be used in practice; it must be truncated. An upper restriction on the kinetic energy of the plane waves can be used to limit the number of them. We refer to this limit as the energy cut-off, or  $E_{cut}$ .

## 2.9. Energy Cutoffs and K-points Sampling

Our lengthy discussion of  $k$  space began with Bloch's theorem, which tells us that solutions of the Schrödinger equation for a super cell have the form

$$\psi_k(r) = e^{ik \cdot r} u_k(r) \quad (14)$$

Where  $u_k(r)$  is periodic in space with the same periodicity as the supercell. It is now time to look at this part of the problem more carefully. The periodicity of  $u_k(r)$  means that it can be expanded in terms of a special set of plane waves:

$$u_k(r) = \sum_G C_{iG} e^{iG \cdot r} \quad (15)$$

Where the summation is over all vectors defined by  $G = n_1 b_1 + n_2 b_2 + n_3 b_3$  with integer values for  $n_i$ . These set of vectors defined by  $G$  in reciprocal space are defined so that for any real space Lattice vector  $l$ ,  $G \cdot l = 2\pi n$ : Combining the two equations above gives

$$\psi_k(r) = \sum_i \sum_G C_{i,k+G} e^{i(k+G) \cdot r} \quad (16)$$

This equation states that the evaluation of the solution at any given location in  $k$  space requires summing over an unlimited set of possible values for  $G$ . This does not seem like it will work well for real-world computations! Fortunately, the functions shown in the previous equation may be understood simply as kinetic energy solutions to the Schrodinger equation.

$$E = \frac{\hbar^2}{2m} |k + G|^2 \quad (17)$$

It makes sense to assume that solutions with lower energy will have greater physical significance than those with very high energies. Consequently, the infinite sum above is typi-

cally truncated to only contain solutions whose kinetic energy is smaller than a certain value:

$$E_{cut} = \frac{\hbar^2}{2m} G_{cut}^2 \quad (18)$$

The infinite sum then reduces to

$$\psi_k(r) = \sum_{|G+K| < G_{cut}} C_{G+K} e^{i(k+G) \cdot r} \quad (19)$$

For varying values of  $k$ , this phrase contains a slightly variable number of terms. The cutoff energy, or  $E_{cut}$ , has been added as a new parameter that needs to be defined each time a DFT computation is done. This parameter is much simpler to define than the  $k$ -points because most packages will use sensible default values in the event that the user provides no additional information. Similar to  $k$ -points, it is advisable to disclose the cutoff energy utilized in your computations to facilitate easy replication of your findings (I.J. Robertson and M.C. Payne, 1990).

In 1976, Monkhorst and Pack devised the most extensively utilized solution. Using these methods one can obtain an accurate approximation for the electric potential and the total energy of an insulator or semiconductor by computing the electronic states at a relatively small number of  $k$ -points. If the system is metallic, the calculation of the electric potential and total energy is more challenging since a dense set of  $k$ -points is needed to correctly characterize the Fermi surface. By choosing a denser set of  $k$ -points, the extent of any inaccuracy in the total energy caused by insufficient  $k$ -points sampling may always be minimized. As the density of  $k$ -points rises, the estimated total energy will converge and the error resulting from the  $k$ -point sample will become closer to zero. In theory, as long as there is computational time available to calculate the electronic wave functions at a dense enough set of  $k$ -points, a converged electronic potential and total energy can always be obtained. The  $k$ -point total energy technique can greatly minimize the computational cost of carrying out a highly dense sample of  $k$ -space. To describe energy cutoff and key points are Basis Sets for Plane Waves is the electronic wave functions at each  $k$ -point can be enlarged in terms of discrete plane-wave basis sets, according to Bloch's theorem. Expanding the electronic wave function theoretically requires an unlimited plane wave basis set. On the other hand, tiny kinetic energy plane wave coefficients are usually more significant than big kinetic energy ones. Consequently, it is possible to truncate the plane wave basis set such that it only consists of plane waves whose kinetic energies are less than a given cutoff energy. No matter how tiny the cutoff energy, the basis set would be infinitely enormous if a continuum of plane wave basis states were needed to extend each electronic wave function. The electronic wave functions can be enlarged in terms of a discrete collection of plane waves by using the Bloch theorem. A finite basis set is created when any energy cutoff is added to a discrete plane wave basis set. An inaccuracy in

the estimated total energy will result from the truncation of the plane wave basis set at a finite cutoff energy. Nonetheless, by raising the cutoff energy value, the error's magnitude might be lessened. The cutoff energy should, in theory, be raised until the estimated total energy converges. Pseudo potential are the first advancements in plane-wave techniques; it has been evident that there may be significant benefits to computations that reduce the amount of plane waves required in a calculation by approximating the properties of core electrons. Using pseudo potential is the most significant way to lessen the computational load caused by core electrons. Conceptually, a pseudo potential substitutes a smoothed density selected to match several significant physical and mathematical aspects of the genuine ion core for the electron density from a selected set of core electrons. This frozen core approximation fixes the characteristics of the core electrons in an approximate way for all further calculations. All-electron computations are those that don't need a frozen core and are far less common than frozen core techniques. An isolated cell of a single element is used to create pseudo potential, but the resulting pseudo potential doesn't need to be adjusted further in order to be utilized successfully for calculations that place this cell in any chemical environment. The transferability of the pseudo potential is the name given to this desired characteristic. A given pseudo potential specifics specify an energy cutoff that must be taken into account in computations involving cells connected to that pseudo potential. Hard pseudo potential is those that need high cutoff energy; soft pseudo potential is those that are more computationally efficient and have lower cutoff energies. The most popular definition of pseudo potential, known as ultra-soft pseudo potential (USPPs), is based on research done at Vanderbilt. These pseudo potentials, as their name implies, need far lower cutoff energy than other methods [20]. Calculating a Self-consistent Field Self-Consistent Field (SCF) solutions to a many-electron problem were first proposed by D.R. Hartree in 1897–1958 as a means of breaking the state. William Hartree, D.R.'s father, assisted him in resolving the numerical issues related to the SCF problem. Here, we'll concentrate on the subject of SCF in DFT computations. Matrix diagonalization, which entails figuring out the self-consistent solutions to the ensuing Kohn-Sham equation (in cellic units), takes the longest in SCF calculations.

$$\left[-\frac{\nabla^2}{2} + V_{ext}(n(r), r)\right] \psi_i(r) = \epsilon_i \psi_i \quad (20)$$

Where  $\psi_i(r)$  is a wave function,  $\epsilon_i$  is a Kohn-Sham eigenvalue. The external potential

$$V_{ex}(n(r); r) = V_{ion}(r) + V_H(n(r); r) + V_{xc}(n(r); r); \quad (21)$$

Includes the ionic potential  $V_{ion}$ , the Hartree potential  $V_H$  and the exchange-correlation potential  $V_{xc}$ . In DFT the external potential depends only on  $n(r)$  the charge density. The

charge density is given by

$$n(r) = 2 \sum_{i=1}^{n_{occ}} |\psi_i(r)|^2 \quad (22)$$

Where is the number of occupied states, or half the system's valence electron count, and spin multiplicity accounts for the factor of two? The process of solving this problem through self-consistent iterations entails estimating the charge density  $n(r)$  at first, estimating  $V_{ext}$ , and computing the Kohn-Sham equation for the wave function to update the charge density and external potential. The process is then repeated for the new wave function by solving the Kohn-Sham equation until the difference between two successive external potentials is less than a predetermined tolerance, or until the wave functions are almost stationary. Self-consistent Iteration Algorithm is an iterative process; the SCF approach produces a set of wave functions and orbital energies that are consistent with it. It involves the subsequent actions.

1. An approximate estimate of the charge density.
2. Solve  $[-\frac{\nabla^2}{2} + V_{ext}(n(r); r)]\psi_i(r) = \epsilon_i \psi_i(r)$  for wave function  $\psi_i(r)$ ,  $i = 1; 2; \dots$
3. Determine the new density of charge
4. Find the new  $V_H$  Hartree potential.
5. Upgrade  $V_{ion}$  and  $V_{xc}$ .
6. We go back to step 3 to estimate the energy again if the wave function does not meet the proper boundary condition. The computation goes back to step 2 and the newly obtained performs the role of wave functions if the wave function fulfills the appropriate boundary condition [10].

### 3. Materials and Computational Methods

The study was based on understanding the structural and electronic properties of gold doped graphene; an intensive literature review is carried out. The main sources of literature review were the published articles, books, thesis and dissertations. Latex software and computers are additional instruments used to accomplish this thesis. All calculations were performed by using spin-polarized DFT method (Hohenberg, 1964) within the vdW correction 'Grimme-D2' approach is set with PWscf code of Quantum ESPRESSO(QE) package by using plane wave ultra-soft pseudo potential (USSP) which is used for structural and electronic properties of the system. For the analysis structural properties Optimized Norm-Conserving Vanderbilt Pseudo potential called as UPF which is compatible with our QR code. The Local Density Approximation (LDA) and generalized gradient approximation (GGA) with Perdew-Burke-Ernzerhof (PBE) was used for determination of exchange-correlation interactions. The plane wave basis set with a cutoff energy of 30 Rey was used after performing the convergence test. The equilibrium inter-layer distance was obtained by minimization of total energy with respect to distance between layers. To investigate the effect of Au impurities on G hetero-structure, Graphene het-



ero-structure was modeled by a super cell of dimensions  $3 \times 3 \times 1$  as shown in Figure 5. These super cells have a total of 18 C atoms. A vacuum space to the z-axis is set to  $15 \text{ \AA}$  which is to eliminate the interaction between spurious images of the G structures. Integrations over the Brillouin zone (BZ) were sampled based on a Monkhorst-Pack 2D grid, which varies for structural relaxation and density calculation depending on the size of the super cells. After structural optimization the calculations were held for pure, and doping was managed by replacing one to two C atoms from G with Au. All data analysis was made using gnu plot, and python code. In addition to this input structures were also visualized using XcrysDen code.

### 3.1. Design Model

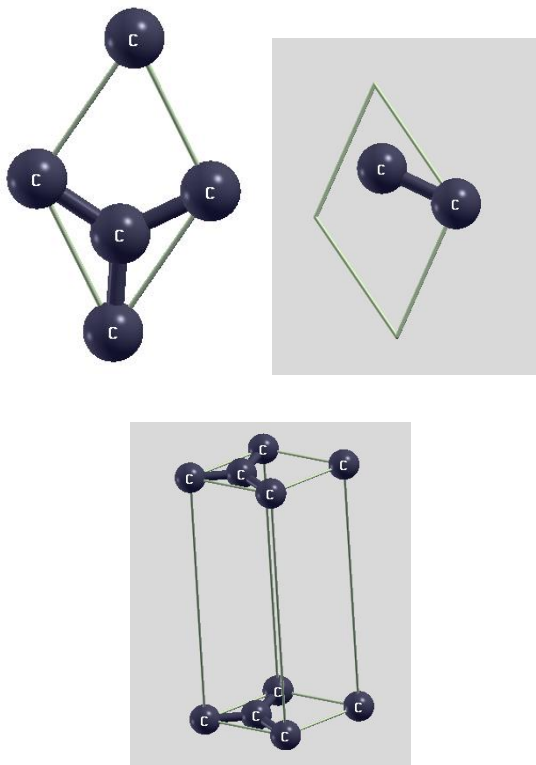


**Figure 5.** Quantum ESPRESSO Logo, unit cell of graphene, translational asymmetric unit of graphene and Supercell respectively.

### 3.2. Flow Chart in DFT

The general Algorithm used to calculate all parameters are summarized in figure [18].

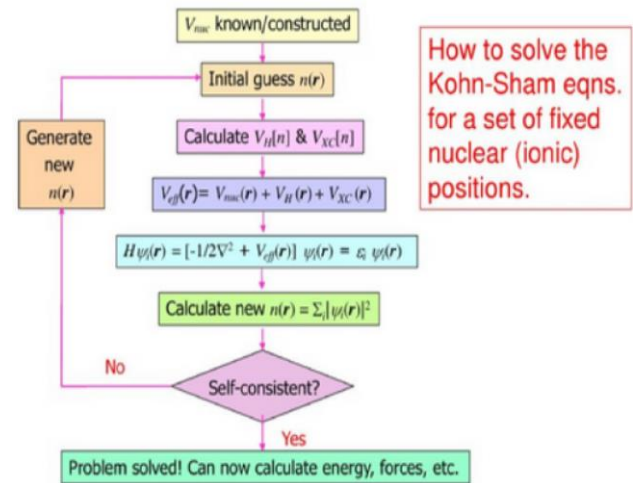


**Figure 6.** Kohn-sham equation iteration to self-consistent field (scf loop).

## 4. Results and Discussion

Results and Discussion make sure that the system is in equilibrium before presenting any results. The structural and electrical characteristics of graphene were calculated in this work using the density functional theory framework. Calculating the equilibrium parameters of the system that correspond to the minimal energy can be achieved, for example, by minimizing the energy. Thus, total energy vs. kinetic energy cut-off and total energy versus the lattice constants of the set are used to verify the convergence of the system.

The total energy was one of the key findings of graphene study. The findings are mostly displayed in three sections of tables and figures. The total energy of graphene with regard to cutoff energy is shown in the first section, and the equilibrium Lattice constant is presented in the second section. And the band structure and density of state of graphene and gold doped graphene are covered in the final section. The output files of the computations were used to deduce the tables of energy cutoffs, and lattice constants against the total energies and graphs were plotted to obtain the optimized parameters for graphene and gold doped graphene.

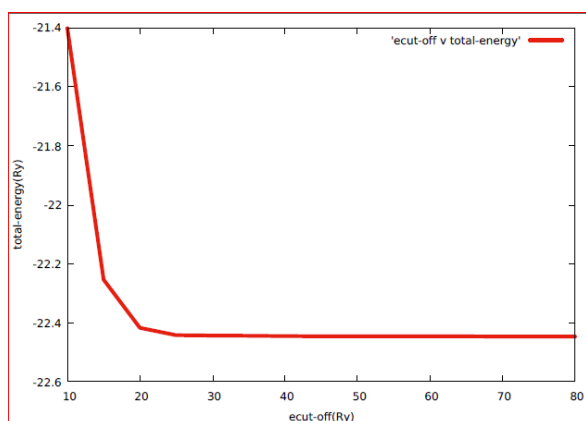
### 4.1. Total Energy of Graphene Per Cell with Respect to Energy Cutoffs

*Convergence Test for the Total Energy with Respect to Cutoff Energy*

**Table 1.** Ecut-off versus total energy.

| N <sub>o</sub> | Ecut-off | total energy | N <sub>o</sub> | Ecut-off | total energy |
|----------------|----------|--------------|----------------|----------|--------------|
| 1              | 10       | -21.40223004 | 9              | 50       | -22.44569997 |
| 2              | 15       | -22.25394531 | 10             | 55       | -22.44575559 |
| 3              | 20       | -22.41671034 | 11             | 60       | -22.44578094 |
| 4              | 25       | -22.44159603 | 12             | 65       | -22.44586829 |
| 5              | 30       | -22.44293027 | 13             | 70       | -22.44604511 |
| 6              | 35       | -22.44373620 | 14             | 75       | -22.44629230 |
| 7              | 40       | -22.44476732 | 15             | 80       | -22.44643113 |
| 8              | 45       | -22.44552915 |                |          |              |

It was determined how much energy graphene had overall as a function of cutoff energy. Until convergence is reached, the total energy of graphene is falling monotonically with rising energy cutoff. The ground state energy was at -22.44275416Ry, and the total energy converges to 30Ry plane wave cutoff energy. The following graphic displays the plot of the cutoff energy and the total energy:

**Figure 7.** Ecut-off vs. total energy.

**Figure 7** Total energy of graphene with a lattice constant of 2.380 Å using Gama k-points as a function of the cut-off energy.

The Lattice constant in this computation is 2.380, and the input parameters are  $2 \times 2 \times 2 = 8$  cells. Different energy cutoff values, ranging from 10Ry to 80 Ry, were utilized to calculate the total energy of graphene per cell relative to the cutoff energy. The resulting total energies were then displayed in the table below. **Figure 7** shows computed total energy of graphene with respect to the cut-off energy. Higher cut-off energies result in slightly lower energies, almost beginning at 30Ryd. But eventually, the variations get very little and have no bearing on how accurate the findings are. In order to lower

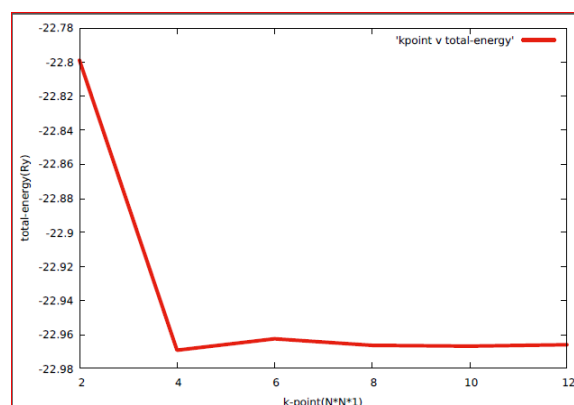
the computational cost, we therefore select cut-off energy of 30Ryd.

## 4.2. Total Energy of Graphene Per Cell with Respect to Energy k-point

*Convergence Test for Total Energy of Graphene*

**Table 2.** k-point versus total energy.

| N <sub>o</sub> | k-point(N*N*1) | total energy(Ry) |
|----------------|----------------|------------------|
| 1              | 2*2*1          | -22.79900257     |
| 2              | 4*4*1          | -22.96918860     |
| 3              | 6*6*1          | -22.96247673     |
| 4              | 8*8*1          | -22.96633892     |
| 5              | 10*10*1        | -22.96677087     |
| 6              | 12*12*1        | -22.96597653     |

**Figure 8.** K-point vs. Total Energy.

For k-point sampling, a convergence test of total energy was run on graphene. The Co cell's total energy was computed with multiple sets of values ranging from  $2 \times 2 \times 1$  to  $12 \times 12 \times 1$ . The plane wave kinetic energy cutoff of 30Ry was used in each of these situations. The PWscf code is used to determine the total energy of graphene as a function of grid size.

The other variables, including the energy cutoff and lattice constant, are held constant for these computations. The total energy reaches a convergence at  $8 \times 8 \times 1$  k-point grids, and its plot is displayed below. The total energy at this point is -22.96633892Ry.

## 4.3. The Equilibrium Lattice Constant of Graphene

By maintaining the k-point grids at  $8 \times 8 \times 1$  k-points and the cutoff energy at 30Ry, the equilibrium lattice constant of

graphene was computed. The lattice parameter was changed in this computation from 2.000 to 3.500 in steps of 0.06 to

determine the total energy of graphene. The output is displayed in the table below.

**Table 3.** Lattice parameter Vs total energy.

| Nº | Lattice parameter | total energy | Nº | Lattice parameter | total energy |
|----|-------------------|--------------|----|-------------------|--------------|
| 1  | 2.406             | -22.97527856 | 13 | 2.478             | -22.98120330 |
| 2  | 2.412             | -22.97651999 | 14 | 2.484             | -22.98090895 |
| 3  | 2.418             | -22.97760663 | 15 | 2.490             | -22.98051767 |
| 4  | 2.424             | -22.97852824 | 16 | 2.496             | -22.97997264 |
| 5  | 2.430             | -22.97930843 | 17 | 2.502             | -22.97937146 |
| 6  | 2.436             | -22.98000110 | 18 | 2.508             | -22.97864385 |
| 7  | 2.442             | -22.98052014 | 19 | 2.514             | -22.97782360 |
| 8  | 2.448             | -22.98093988 | 20 | 2.520             | -22.97686795 |
| 9  | 2.454             | -22.98120373 | 21 | 2.526             | -22.97581236 |
| 10 | 2.460             | -22.98136259 | 22 | 2.532             | -22.97467324 |
| 11 | 2.466             | -22.98141049 | 23 | 2.538             | -22.97344546 |
| 12 | 2.472             | -22.98139317 |    |                   |              |

The Equilibrium Lattice with Constant k-point grids of k-point  $8 \times 8 \times 1$ , a constant cutoff energy of 30Ry, and various choices of lattice parameters ranging from 2.000 to 3.500, the total energy of graphene was calculated.

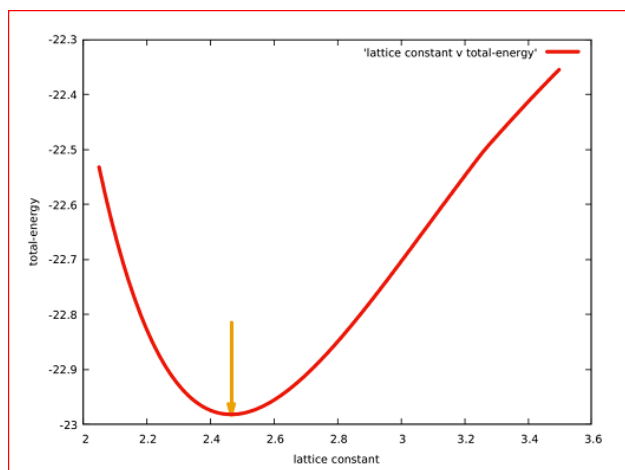


**Figure 9.** Lattice parameter vs. Total Energy.

**Figure 9** Total energy of graphene with  $E_{\text{cut}}=30$  Ryd and  $8 \times 8 \times 1$  k-points as a function of the lattice parameter,  $a$ . **Figure 8** illustrates the fluctuation of total energy with a few values of the lattice constant as for the  $8 \times 8 \times 1$  k-points and  $E_{\text{cut}} = 30$  Ry. By fitting the data to the cubic spline curve in accordance with

usual procedure (Castro E. V., 2010), we were able to find the equilibrium lattice constant at  $2.476 \text{ \AA}$ , which corresponds to the lowest energy value. In order to confirm the accuracy of this calculated value  $a$ , we computed total energy over a wide range of values, from 2.00 to  $3.500 \text{ \AA}$ . The outcomes are displayed in **Figure 6** amid the numerical fluctuations of computed values, we observe that the energy minimum is reached at  $a = 2.476 \text{ \AA}$ .

As a result, we determine that our numerical estimate's error margin is  $0.016 \text{ \AA}$ . Thus,  $a = (2.460 \pm 0.016) \text{ \AA}$  is our numerical estimate of  $a$ . Insulators and semiconductors behave well in terms of k-integration in that the integration of a smooth function typically does not result in issues and the density of states approaches zero smoothly before the gap. In the case of metals, however, it might be quite difficult to resolve the functions that need to be integrated in plane waves; the functions must first be multiplied by a severe Fermi occupancy. The graphene unit cell (A) and translational asymmetric unit (B) are shown in **Figure 8**. The crystal lattice constant,  $a$ , is set as the parameter in the plane at  $a = 2.476 \text{ \AA}$ .  $1.4217 \text{ \AA}$  is the length of the C-C bond. Using extremely soft pseudo-potentials and the local density approximation (LDA), the calculations were carried out within the context of DFT. Due to the fact that computations using the generalized gradient approximation (GGA) produce values of  $C$  that are far too high and almost no bonding between graphene planes (Ooi N, 2006).

#### 4.4. Structural Property of Pure and Gold Doped Graphene

To manage doping, first we have extended the unit cell to super cell by duplicating the unit cell along x and y. For this study we have used  $3 \times 3 \times 1$  super cells, which contain 18 carbon atoms as shown from Figure 7.

*Lattice parameter, bond length, bond angle*

After structural optimization, the calculated bond length of the unit cell of C-C = 1.4249 Å, which is in agreement with experimental reported value C-C = 1.42 Å (Vorontsov, 2018) (Gong, 2011). The optimized and relaxed stable super cell of graphene and Au are joined to form the hetero-structure  $3 \times 3 \times 1$  (containing 18 C atoms, 1 Au atoms) and investigated

in this study. We calculated the in-plane lattice parameters for pure G to be 2.476 Å, graphene to be 2.468 Å as shown in Figure 7 above. The crystal of a super cell of pure G hetero-structures for layers' bond angles between C-C-C is  $120^\circ$  using simple geometry. When the single carbon atom is replaced by the Au atom, the structure is somewhat deformed as a result of the stress that the dopant atom causes, as illustrated in Figure 9. Thus, the lattice constant of G-Au increased from 2.48 Å to 2.7902 Å on Graphene layer, while the bond length of C-C extended from 1.4318 Å to 1.8593 Å and bond angle C-C-C decreased from  $120^\circ$  to  $90:94^\circ$  for C-Au-C. Table 4. The effect of Au doped on bond length, bond angle, and lattice constant of G hetero-structure around the dopant; is experimental value (ex.val).

**Table 4.** The effect of Au doped on bond length.

| System                | Type     | Bond Length(Å) |        | bond angle( $^\circ$ ) |        | lat. co.( Å) | ex.val.(Å) |
|-----------------------|----------|----------------|--------|------------------------|--------|--------------|------------|
|                       |          | C-C            | C-Au   | C-C-C                  | C-Au-C |              |            |
| $3 \times 3 \times 1$ | Pure     | 1.42           |        | 120                    |        | 2.476 Å      | 2.46 Å     |
| $3 \times 3 \times 1$ | Au-doped |                | 1.7964 | 124.3                  | 120    |              |            |

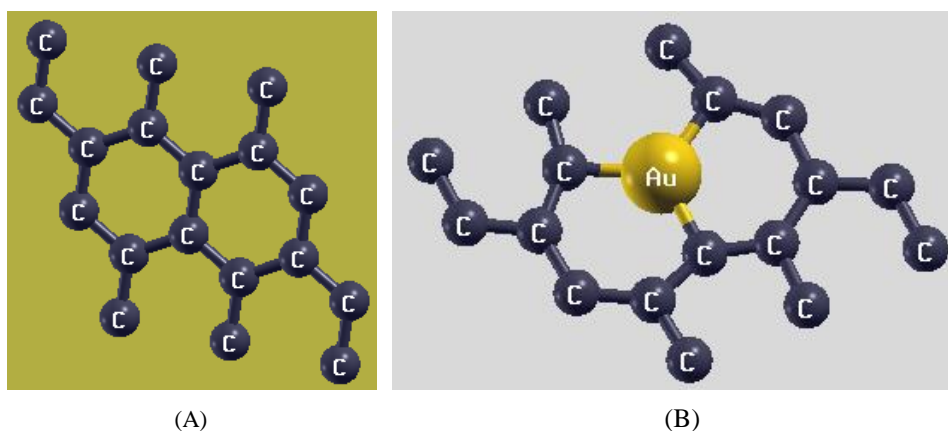


**Figure 10.** Model of G heterostructures for (a)  $3 \times 3 \times 1$  pure and (b)  $3 \times 3 \times 1$  Au-doped graphene.

#### 4.5. The Effect of Au Doping on Electronic Properties of Pure G Hetero-structure

Under this section we have discussed the effect of Au doping on electronic properties of pristine G hetero-structure from the plots of total density of states (TDOS), partial density of states (PDOS) and band structure.

The total density of states (TDOS) and projected density of states (PDOS) for undoped and Au-doped G hetero-structure were plotted to help understand how the states are spread and which electronic orbits are more important for electronic and

magnetic transport. Figure 10 illustrates the symmetric nature of TDOS for spin-up and spin-down channels. Therefore, it may be concluded that these materials have a nonmagnetic semiconductor nature based on the symmetric behavior of the spin up and spin down channels of TDOS. When an Au dopant is present, the spin degeneracy of TDOS is broken, and some additional states are generated in spin-up DOS that cross the Fermi level and expose the metallic behavior, while in spin-down DOS, no states cross the Fermi level and reveal the semiconductor behavior of spin down states.

*DOS for 3x3 pure Graphene*



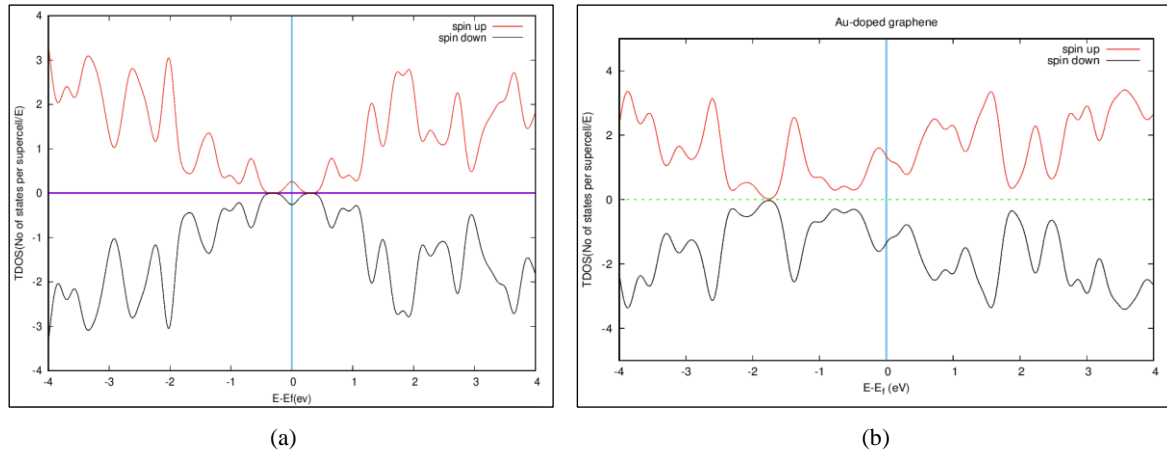


**Figure 11.** Total density of states (TDOS) for (a)  $3 \times 3 \times 1$  pure (b)  $3 \times 3 \times 1$  Au-doped Graphene.

Furthermore, the partial density of states (PDOS) for the unpolluted and Au-doped G heterostructures was displayed in order to clearly determine which orbital is more responsible for the electronic properties. According to Figure 11, for pure G heterostructures, carbon P-orbital is responsible for the

majority of the contributions to the state at Fermi level. For a single Au-doped G, however, the drive from Au 5d orbital electrons is the dominant contributor close to the Fermi level as indicated in figure 12.

3x3 G pure PDOS

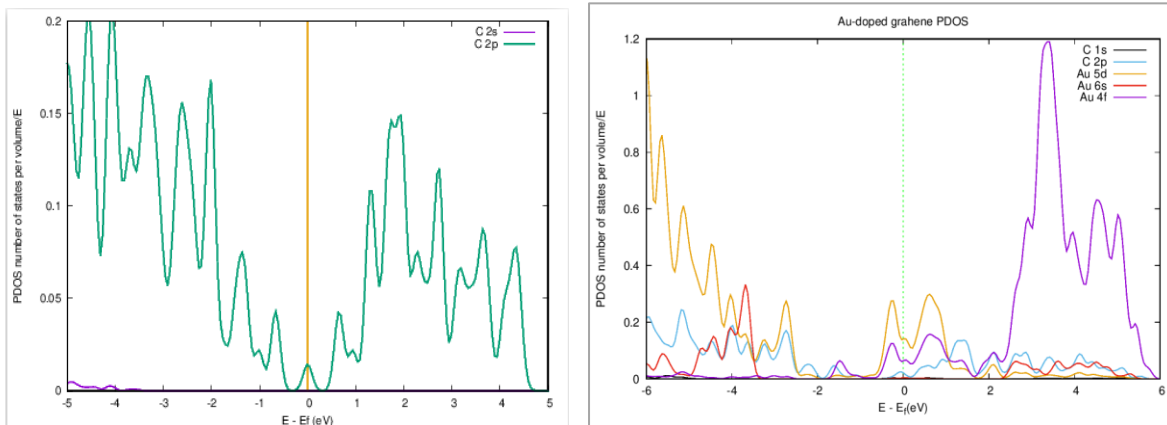


**Figure 12.** Partial (projected) density of states for (a)  $3 \times 3 \times 1$  pure (b)  $3 \times 3 \times 1$  Au-doped graphene.

Figure 12 displays the Au doped graphene's predicted partial density of states (PDOS) and total density of states (TDOS). For Au doped graphene structures, the largest peaks at the Fermi level are seen in the occupied region due to the p orbital of graphene. P orbitals from the C atom dominate the density of states above the Fermi level, while the contributions of the p orbitals from the Au and C atoms are about equal. Figure 11 Demonstrates that orbital hybridization can be seen for the C-Au-doped graphene systems close to Fermi energy, which may indicate the possibility of metallic characteristics. P orbitals of Au and C atoms are the primary contributors to the density of state at the Fermi level.

Band Structure of Pure and Au-Doped Graphene are Energy band structures for pure and single Au- doped in  $3 \times 3 \times 1$  and were plotted in order to better understand the band gap's characteristics as well as the impact of Au-doping on energy

band structure. Figure 13 illustrates how the valence band maximum (VBM) and conduction band minimum (CBM) of the pure and doped 2D hexagonal BZ systems are localized at K-high symmetry sites, showing that the band gap is direct in nature.

Electronic band structure of pristine graphene

The graphene band structure is depicted in Figure 13. The conclusion in the literature (McCann E. and Fal'ko V. I., 2006) is supported by the observation that the two bands appear to contact at the K point, indicating that the graphene is semiconductor. The bands, which are created by combining the p orbitals of the two bases of C atoms in each primitive hexagonal unit cell, are shown by the electron dispersion curves in Figure 13. At the Fermi level, For both the electron and the hole bands, the dispersion around the K point is linear. The electron resides in the p orbital, where it overlaps with the

nearby carbon atoms p electron to form a bond. This electron is delocalized throughout the lattice and has a higher energy than the electrons that form the bonds. These delocalized electrons govern Graphene's electrical characteristics.

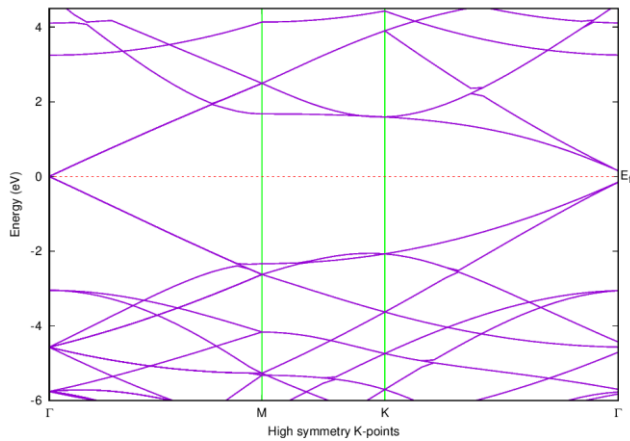


**Figure 13.** Electronic band structure of pristine graphene at the direction of  $\Gamma$ MKT.

The entire density of states for pure graphene is shown in Figure 10. It is evident that at the Fermi energy, the DOS plot shows no band gap (or, conversely, no overlap between the conduction and valence bands). Wallace et al. also disclosed this attribute (P. R. Wallace, 1947). The connecting of the valence and conduction bands at the Brillouin zone's  $\Gamma$ -point, at the bottom of the Fermi energy, results in the absence of a band gap. In theory, pure graphene is revealed to be a semiconductor when it has a zero-band gap. Au-doped graphene is used in Figure 10 unit cell of the final relaxed configurations to create an  $8 \times 8 \times 1$  super cell structure.

In the x-y plane, the super cell parameters are set to  $a = b = 7.428 \text{ \AA}$ , where  $a$  and  $b$  are the crystal lattice constants. In ideal bilayer graphene, the relaxed Au-C bond length is  $1.432 \text{ \AA}$ . Using ultra soft pseudopotential and the local density approximation (LDA), the computations were carried out within the DFT framework.

#### Band structure of Au doped graphene

The band structure of Au doped graphene constructed in an  $8 \times 8 \times 1$  super cell is depicted in Figure 14. The inclusion of Au impurities disrupts the band crossover of pure graphene. The Fermi level has now been pushed to the conduction band, indicating that the graphene and Au dopant are interacting and rendering the graphene semi-metallic. The Au dopant has clearly altered the bands, particularly in the area above or below the Fermi level. A thorough examination reveals that the band of  $E_f$  at gamma is localized on Au in the s-orbital, but it is localized on graphene around K point, which is located directly below  $E_f$ . Figure 10 unit cell of final relaxed configurations Au doped graphene.

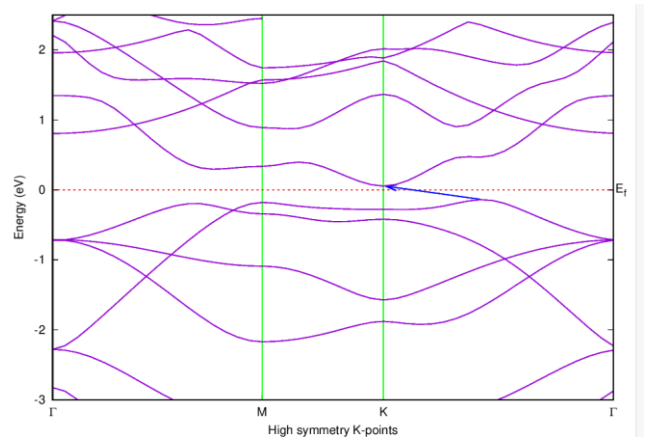


**Figure 14.** Electronic band structure of Au doped graphene at the direction of  $\Gamma$ MKT.

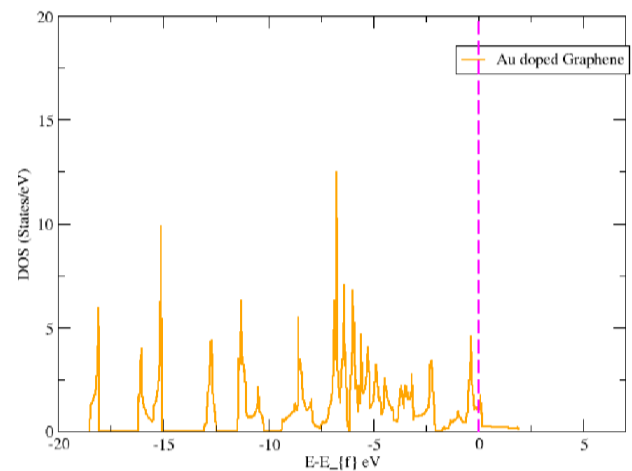


**Figure 15.** Density of state for Au doped graphene.

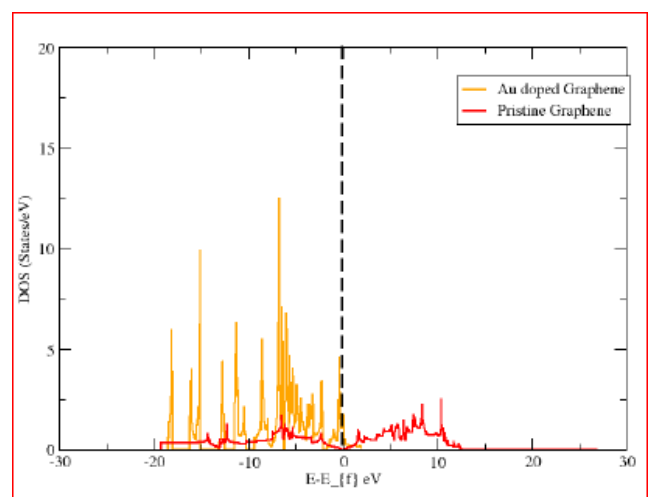


**Figure 16.** Density of state for Au doped graphene.

At the Fermi level, the corresponding DOS in Figure 15. exhibits a strong peak. Therefore, graphene becomes semi-metallic due to the Au doping. The difference in DOS

between pristine and Au-doped graphene is shown in Figure 16. The graph illustrates that Au doped graphene exhibits a higher metallicity compared to virgin graphene, as seen by the graph's largest peak at the Fermi level.

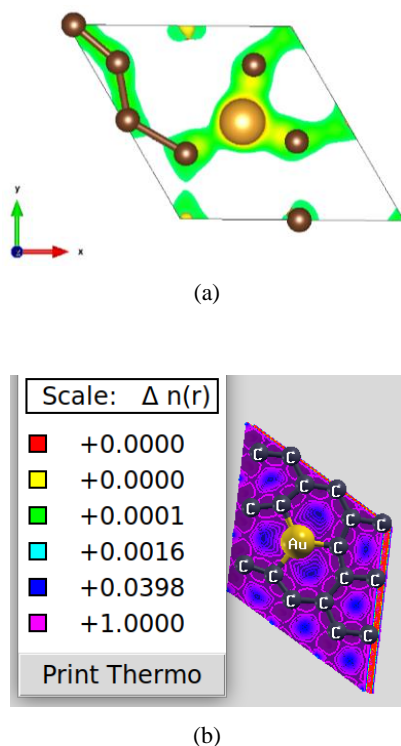


**Figure 17.** The charge density isoface of graphene.

Figure 17 displays the charge density distributions on the planes that cross the carbon atoms in graphene and the Au atom. Electrons surrounding the Au atom in graphene exhibit localized features in Au-doped graphene. (Castro E. V., 2010). Reportedly examined the nature of vacancy-induced electronic states in bilayer graphene. It was shown that the wave function was completely delocalized in one stratum and quasi-localized in another. They observed that the delocalization resulted from the wave function spreading onto the layer across from where the vacancy was located.

Moreover, the Au-C interaction exhibits greater values of the charge density between the doped Au atom and the carbon atoms, as seen in Figure 17, clearly demonstrating a covalent-bonding character.

In Figure 17, the red and pink parts indicate the low and high electron numbers, respectively. When Au atoms are doped into graphene, in graphene, some of the electrons on the hybridized orbitals of Au atoms are trapped in the hybridized orbitals of C atoms, while the electron density around the Au atoms is reduced. However, the increase in the electron density around the C atoms in graphene is evident. It shows that electrons are transferred from the orbitals of Au atoms to those of C atoms.

## 5. Conclusions and Recommendations

### 5.1. Conclusion

In this study, we employed density functional theory with a local approximation to conduct plane wave pseudo-potential calculations; focusing on the electronic structure of gold (Au) doped graphene. Our results demonstrate a clear transition from semi-metallic to metallic behavior due to the doping process. We identified the top site on the graphene sheet as the optimal position for Au doping, based on the variation in doping energies across different locations on the graphene lattice. Within an 8x8x1 graphene super cell, we found that the equilibrium distance of the Au atom from the graphene surface is 1.432 Å, which is consistent with previous findings (Vorontsov, 2018). The incorporation of a single Au atom notably alters the structural properties of the monolayer graphene supercell. Band structure analysis reveals that pure graphene features conduction and valence bands that converge at the Fermi level, classifying it as a zero-band gap semiconductor. Furthermore, our investigation indicates that the introduction of an Au atom results in semiconductor behavior, characterized by a small band gap between the valence and conduction bands. The density of states (DOS) analysis for pure graphene confirms its semi-metallic nature, while the properties of Au-doped graphene highlight how Au doping significantly influences its electronic characteristics, allowing it to retain its semi-metallic behavior.

### 5.2. Recommendations

In this study, we utilized density functional theory (DFT) to explore the structural and electronic properties of 3x3x1 super cell systems, which were limited by the availability of supercomputing resources and time constraints. For future work, we recommend increasing both the super cell size and impurity concentrations to gain deeper insights. Additionally, we aim to conduct a thorough investigation of the structural and electronic properties using DFT + U to enhance our understanding of these systems.

## Abbreviations

|         |  |
|---------|--|
| 2D      | Two-Dimensional  |
| Au      | Gold   |
| BZ      | Brillion Zone  |
| DFT     | Density Functional Theory                                  |
| DOS     | Density of States  |
| G       | Graphene   |
| GGA     | Generalized Gradient Approximation                         |
| GGA-PBE | Generalized Gradient Approximations-Perdew Burke Ernzerhof |
| HCP     | Hexagonal Close Packed                                     |
| KS      | Kohn Sham  |
| PDOS    | Projections of Density of States                           |

|       |                                  |
|-------|----------------------------------|
| PP    | Pseudo Potential                 |
| PWSCF | Plane-Wave Self-Consistent Field |
| QE    | Quantum ESPRESSO                 |
| QM    | Quantum Mechanical               |
| SCF   | Self-consistent Field            |
| US-PP | Ultra Soft Pseudo-Potentials     |
| XC    | Exchange-Correlation             |

## Conflicts of Interest

The authors declare no conflicts of interest.

## References

- [1] B. G. Pfrommer, M. S. (1997). "Relaxation of Crystals with the quasi-Newton method," J. Comput. Phys. 131(1).
- [2] L. Brey and H. A. Fertig, Phys. Rev. B 73, 235411 (2006).
- [3] C. Fiolhais, F. N. (2003). "A Primer in Density Functional Theory". Springer-Verlag Berlin. C. Lee, X. W. (2008). *Science* 321. *Science* 321.
- [4] Castro Neto AH et al. (2009). *The electronic properties of graphene*. Rev. Mod. Phys. 81. 109-62.
- [5] Compton OC and Nguyen S B T. (2010). *Graphene oxide, highly reduced graphene oxide, and graphene: versatile building blocks for Carbon based materials Small*. 6 711-23.
- [6] Cooper D. R., D. A. (2012). *Experimental review of graphene*. International Scholarly Research Notices.
- [7] Cooper, D. R., D'Anjou, B., Ghattamaneni, N., & al., e. (2012). "Experimental Review of Graphene", International Scholarly Research Network.
- [8] D M. Ceperley and B. J. Alder. (1980). "Ground state of the electron gas by a stochastic method". Phys. Rev. Letters. Vol. 45.
- [9] D. Vanderbilt. (1990). "self-consistent pseudopotentials in a generalized eigenvalue formalism". Physical Review, Vol. 41.
- [10] D. S. Sholl, J. S. (2009). "Density Functional Theory a Practical Introduction". Vol. 1 John Wiley and Sons.
- [11] Dai J, Y. J. (2009). *Gas adsorption on graphene doped with B, N, Al, and S: a theoretical study*. Appl. Phys. Lett. 95 183.
- [12] Dean, C. Y. (2010). *For high-quality graphene electronics*. Nature nanotechnology, 5(10).
- [13] E. Lipparini. (2003), "Modern Many-Particle Physics: Cellic Gases, Quantum Dots and Quantum Fluids,". Singapore, World Scientific.
- [14] F. Rioux. (1991). "A Hartree self-consistent field calculation on the helium cell". Eur. J. Phys. Vol. 12.
- [15] Fatemeh Farjadian, S. A. (2020). *Recent Developments in Graphene and Graphene Oxide: Properties, Synthesis, and Modifications: A Review*, <https://doi.org/10.1002/slct.202002501>
- [16] G. Vignale and M. Rasolt. (1987). "Density-functional theory in strong magnetic fields". Physics Review Letters, Vol. 59.
- [17] Giannozzi, P. B. (2009). *QUANTUM ESPRESSO: a modular and open-source software project for quantum simulations of materials*. Journal of physics: Condensed matter, 21(39).
- [18] Grimme, S. (2004). *Accurate description of van der Waals complexes by density functional theory including empirical corrections*. Journal of computational chemistry, 25(12).
- [19] J. Hafner, C. W. (2006). "Toward Computational Materials Design: The Impact of Density Functional Theory on Materials Research". Mrs bulletin, Vol. 31.
- [20] Roberts, M. C. (2010). *Continuum plate theory and atomistic modeling to find the flexural rigidity of a graphene sheet interacting with a substrate*. Journal of Nanotechnology.
- [21] Schrodinger, E. (1926). "Quantisierung als Eigenwertproblem". Annalen der Physik, Vol. 385.
- [22] Ham, W. K. (1965). *Self-consistent equations including exchange and correlation effects*. Physical Review 140 (4A).
- [23] S. Some S, K. J. (2012). *Highly air-stable phosphorus-doped n-type graphene field-effect transistors*. Adv Mater. 24: 5481.
- [24] Somnath Bharech and Richa Kumar. (2016). *A Review on the Properties and Applications of Graphene*. Review.